

Self-Powered Microscale Pumps Based on Analyte-Initiated Depolymerization Reactions**

Hua Zhang, Kimy Yeung, Jessica S. Robbins, Ryan A. Pavlick, Meng Wu, Ran Liu, Ayusman Sen,* and Scott T. Phillips*

Microscale pumps that are simultaneously capable of turning “on” in response to specific analytes in solution and of providing precise control over flow rate will be needed for certain types of smart micro- and nanoscale devices. Access to these types of pumps, however, has remained limited.^[1] Two general approaches for designing microscale pumps have been proposed:^[1–3] 1) those that are turned on and off by input from the user; and 2) single-use pumps that are turned on autonomously by exposure to a specific chemical signal, and therefore do not need to be turned off. The ideal pump in this second category would combine sensing and pumping capabilities, and thus would enable pumping that is controlled by the presence and concentration of a specific analyte. Herein we describe the first examples of this second type of microscale pump. We characterize this type of pump, and establish both the chemical and physical–chemical foundation upon which future applied efforts will be based.

The pumps consist of insoluble polymer films that depolymerize to release soluble monomeric products when exposed to a specific analyte (Figure 1).^[4,5] Products formed as a result of the depolymerization reaction amplify the signal^[5] and create a concentration gradient that pumps fluids (and insoluble particles) away from the bulk polymer owing to a diffusiphoretic mechanism. These pumps are self-powered, are capable of turning “on” in response to specific analytes, and can be tuned to respond to a variety of analytes ranging from small molecules to enzymes. They also provide pumping velocities ranging from $0.1 \mu\text{m s}^{-1}$ at low concentrations of analyte up to $11 \mu\text{m s}^{-1}$ at high concentrations of analyte. Moreover, the pumps are capable of moving fluids and insoluble micrometer-scale particles directionally despite viscous drag in low Reynolds number regions,^[6] and despite Brownian randomizations.^[3a,7]

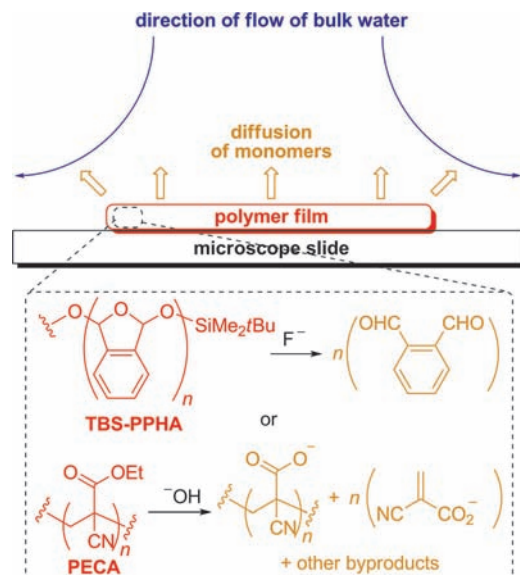


Figure 1. Design of self-powered micrometer-scale pumps that are based on analyte-induced depolymerization of individual polymers within a polymer film. Films were made from either *tert*-butyldimethylsilyl (TBS) end-capped poly(phthalaldehyde) (TBS-PPHA), which depolymerizes in response to fluoride,^[5] or poly(ethyl cyanoacrylate) (PECA), which responds to base.^[8]

To demonstrate these types of pumps, we prepared micrometer-scale polymer films on glass slides. The films were composed of a polymer that is capable of depolymerizing when it responds to a specific chemical signal. We tested two types of polymers: *tert*-butyldimethylsilyl (TBS) end-capped poly(phthalaldehyde)^[9,10] (TBS-PPHA),^[5] which depolymerizes in response to fluoride, and commercially available poly(ethyl cyanoacrylate) (PECA),^[8] which depolymerizes and degrades in response to base (Figure 1).

The type of polymer used for the pumps is important: it affects both the speed and magnitude of the pumping response. For example, typical degradable polymers require a separate reaction with the analyte for release of each repeating unit. TBS-PPHA, in contrast, is a polymer that depolymerizes rapidly (that is, seconds), continuously, and completely from one end of the polymer to the other when the TBS end-cap is cleaved from the polymer by reaction with fluoride.^[5] Thus, TBS-PPHA requires only a single equivalent of fluoride to release 133 monomers (the TBS-PPHA polymer used in this study contained about 133 repeating units, although longer polymers could be used), meaning that a single detection event causes a dramatic increase in the concentration (and therefore gradient) of products in solu-

[*] H. Zhang, K. Yeung, J. S. Robbins, R. A. Pavlick, M. Wu, R. Liu, Prof. A. Sen, Prof. S. T. Phillips
Department of Chemistry, The Pennsylvania State University
University Park, PA 16802 (USA)
E-mail: sphillips@psu.edu
asen@psu.edu
Homepage: <http://research.chem.psu.edu/stpgroup/>
<http://research.chem.psu.edu/axsgroup/>

[**] This work was supported by the NSF (DMR-0820404, CBET-1014673), DARPA (N66001-09-1-2111), the Arnold and Mabel Beckman Foundation, the Camille and Henry Dreyfus Foundation, 3M, Louis Martarano, and the Pennsylvania State University. We appreciate the assistance of Prof. Darrell Velegol (Department of Chemical Engineering) in calculating the power of the pumps.



Supporting information for this article is available on the WWW under <http://dx.doi.org/10.1002/anie.201107787>.

tion. Poly(alkyl cyanoacrylates), in comparison, are a family of biocompatible and biodegradable polymers that are non-toxic and non-immunogenic to the human body.^[11] The mechanism for base-initiated depolymerization/degradation of the PECA polymer backbone proceeds through several pathways, including depolymerization from one end of the polymer to the other, hydrolysis of the side-chain esters, as well as other, less pronounced degradation pathways.^[8,12]

Exposure of these polymer films either to fluoride (TBS-PPHA) or base (PECA) causes depolymerization of the polymers on the surface of the film, thus releasing monomeric products into solution and initiating movement of the water positioned above the film towards the film where there is a high concentration of solute (that is, depolymerization products; Figure 1). Water that moves initially in the z direction towards the film then moves away from the film radially at the surface of the film, thus pumping away

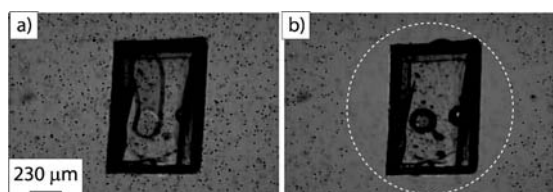


Figure 2. Snapshots of exclusion zones around the TBS-PPHA polymer film caused by analyte-induced radial pumping. The snapshots were taken from Movie S1 in the Supporting Information. The dots in the images are 6 μm diameter polystyrene tracer particles that reveal the movement of the fluid. a) Image taken 0 s after exposure to 0.1 M NaF in distilled water at 25 $^{\circ}\text{C}$, and b) 1000 s after exposure. The dotted line in b) indicates the approximate boundary of the exclusion zone. Movie S1 shows the entire pumping process.

insoluble particles (Figure 2; Supporting Information, Movies S1 and S2).

Figure 2 and Movie S1 show one example of this phenomenon. The images in Figure 2 show a film of TBS-PPHA that is immersed in an aqueous solution (25 $^{\circ}\text{C}$) that contains 6 μm diameter polystyrene tracer particles and 0.1 M NaF. No movement of fluid is observed upon initial exposure to the NaF solution (Figure 2a), but within seconds the tracer particles begin to move radially away from the polymer film to create an exclusion zone around the film (Figure 2b). In the absence of fluoride, the particles do not move (TBS-PPHA does not depolymerize),^[5] and in the presence of 0.1 M NaCl, the average particle velocity is negligible (reaching only 0.1 $\mu\text{m s}^{-1}$), thus verifying the selectivity of the TBS-PPHA pump for fluoride.^[5] When exposed to 0.1 M NaF, the TBS-PPHA pumps are capable of continuous pumping for > 15 min (settling of the 6 μm diameter polystyrene tracer particles onto the surface of the glass slide precluded measurements of longer pumping times).

PECA pumps provide a similar exclusion zone as was observed with the TBS-PPHA pumps, but in this case the pumping response is caused by an aqueous solution of 0.01 M NaOH (Supporting Information, Movie S2). In a control experiment using 0.01 M NaCl instead of NaOH, no zone of

exclusion was observed for the PECA pump. Moreover, the direction of movement of the tracer particles in these types of pumps is independent of the charge of the tracer particle (that is, both negatively charged carboxylate functionalized tracers, as well as positively charged amidine-functionalized tracers, behave similarly; Supporting Information, Movie S3), thus ruling out a pumping mechanism based upon an ionic gradient.

Figure 3a,b further show that the pumping velocity created by these pumps depends on the concentration of the analyte. For example, Figure 3a shows the distribution of particle velocities as a function of the concentration of fluoride that was exposed to a TBS-PPHA pump. The particle velocities in Figure 3a were measured at distances of 100 μm

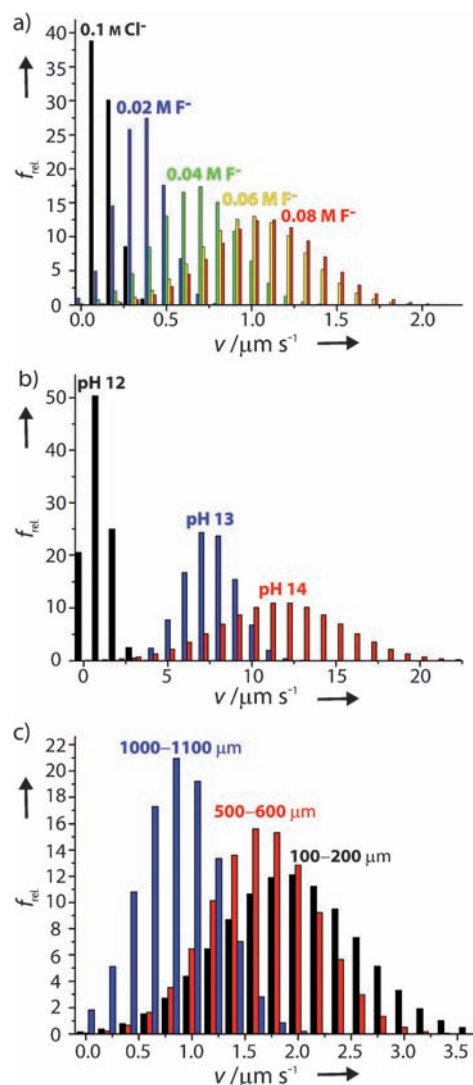


Figure 3. Velocity (v) distributions of tracers. a) Exposure of TBS-PPHA pumps to different fluoride concentrations. b) Exposure of PECA pumps to aqueous solutions with different hydroxide concentrations. c) At different distances from a TBS-PPHA pump when the pump was exposed to 0.1 M NaF at 25 $^{\circ}\text{C}$. The particle velocities in (a) and (b) were measured in the region 100 μm to 200 μm from the pump and from 0 s to 7 s after exposure of the pump to the solution. The particle velocities in (c) were measured over the time period of 5 s to 35 s after exposure to fluoride. The relative frequency of particles is f_{rel} .

to 200 μm from the pump and at time points from 0 s to 7 s after exposure to fluoride. There is a clear Gaussian distribution of particle velocities at each concentration of fluoride over this range of distances and time, yet the average velocities of the particles increased as a function of the concentration of fluoride, reaching an estimated maximum velocity of $1.15 \mu\text{m s}^{-1}$ at 0.1M NaF.

The effect of analyte concentration on pumping velocity was observed with PECA pumps as well (Figure 3b), which reached a maximum average pumping velocity of approximately $11 \mu\text{m s}^{-1}$ in a pH 14 aqueous solution (1M OH^-). This velocity is approximately twice as fast as the average swimming velocity of *Escherichia coli* (*E. coli*) ($5\text{--}7 \mu\text{m s}^{-1}$ at surfaces^[13]).

The pumping velocity for this type of pump, as with all pumps, depends on the distance from the pump where the velocity is measured. Figure 3c shows the change in average particle velocity as a function of distance for a TBS-PPHA pump over the time period of 5 s to 35 s after exposure to 0.1M NaF at 25°C. The data in Figure 3c reveals that the TBS-PPHA pump is capable of providing average pumping velocities of at least $0.8 \pm 0.4 \mu\text{m s}^{-1}$ at distances over 1 mm from the pump.

Our hypothesized mechanism for these pumps is depicted in Figure 1. This mechanism is based on a non-electrolyte diffusiophoretic model in which the concentration gradient of monomeric products above the polymer film leads to movement of water in the z direction from above the film towards the film. This movement of water creates convective flow within the confines of the test container that leads to the movement of water initially in the z direction towards the pump, and then radially away from the pump in the x,y plane.

To test this mechanism, we prepared 2 μm diameter PECA particles (Supporting Information, Figure S1) as a control system to evaluate whether analyte-induced depolymerization would cause enhanced diffusion rates of the PECA particles. Techniques for probing the mechanisms that lead to motion of particles are well established,^[14] therefore we reasoned that control studies using PECA particles, rather than films, might provide further insight into the mechanism of the pumps.

The 2 μm -diameter PECA particles show enhanced diffusivity (see Supporting Information) in basic solutions, which we attribute to the depolymerization reaction and not to the decrease in particle size that results over the course of the depolymerization reaction. As depolymerization is an endothermic, entropy-driven reaction, the enhanced diffusion is not because of local heating. Instead, we propose that the enhanced diffusivity arises from shape asymmetry and surface imperfections in the particles that leads to greater exposure of some areas on the particle to the analyte in solution (Figure 4).

A larger area of exposure should lead to an increase in the number of polymers that depolymerize, causing an uneven increase in the local concentration of monomeric products around the particle and an increased diffusivity owing to a non-electrolyte diffusiophoretic mechanism.^[15,16] This mechanism arises from steric exclusion, which is generated from the products interacting with the particle surface, thus

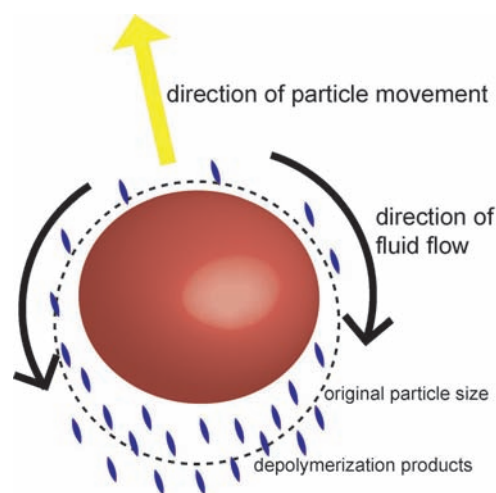


Figure 4. Proposed diffusiophoretic mechanism for enhanced rates of diffusion of 2 μm PECA particles (maroon semi-spherical object) in basic aqueous solutions. Note: As the particles degrade to some extent over their entire surface creating multiple product sources, the generated product gradient across the particle is not likely to be as steep as that shown here in the idealized picture.

creating a pressure gradient along the particle. This pressure gradient drives fluid flow in the direction of higher product concentration, thus pushing the particle in the opposite direction. The depolymerization process is related to the particle velocity (U) by the equation:^[15,16]

$$U = \frac{kT}{\eta} KL \nabla C \quad (1)$$

where k is the Boltzmann constant, T is temperature, η is viscosity, K is the Gibbs absorption length, L is the length of the particle–product interaction, and C is the product concentration. The observed enhanced diffusion coefficient of the PECA particles in the presence of base can be related to the ballistic velocity through the following equation:

$$D^* - D = \frac{U^2}{4D_r} \quad (2)$$

where $D^* - D$ is the net enhancement in diffusion coefficient, U is the particle velocity, and D_r is the rotational diffusion coefficient (for a 2 μm particle D_r is calculated to be 0.23 s^{-1}).^[14,17] Using the relationship described by Equation (2), the calculated velocity of the particles are $0.18 \mu\text{m s}^{-1}$ in pH 8 solution and $0.25 \mu\text{m s}^{-1}$ in pH 8.5 solution. These velocities compare well with the observed pumping velocity for PECA pumps at pH 8 ($0.21 \pm 0.12 \mu\text{m s}^{-1}$). The agreement between the computed particle velocity and the experimental pump velocities lead us to conclude that the same mechanism probably causes both the convective flow of water around the pumps and the enhanced rate of diffusion of the PECA particles.

With an eye towards future applications, we broadened the scope of these new types of autonomous pumps by demonstrating the ability of TBS-PPHA pumps to move

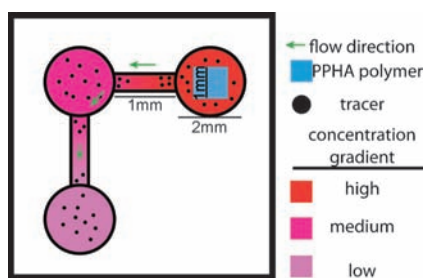


Figure 5. Configuration of a channel to demonstrate that the TBS-PPHA pump is capable of moving particles over distances of about 5 mm and around corners. The gradient of color from red to pink represents an approximation of the concentration of monomer within the channel.

fluids long distances through channels (Figure 5; Supporting Information, Movie S4). In this experiment, we evaluated whether the tracer particles could move from right to left (the pump was positioned on the right), turn left, and then move from right to left again, but in a perpendicular direction in the x,y plane; we also tested whether the particles could be pumped the entire length of the 5 mm-long channel.

Upon exposure to fluoride, the pumping was confined initially from right to left in the top channel, as expected, but over time (that is, presumably once the concentration gradient of the monomeric products increased), the particles in the left chamber turned the corner and started to flow in the second channel, again from right to left, until they reached the end of the channel (Supporting Information, Movie S4). The estimated power for this type of pump is roughly $4 \times 10^{-18} \text{ J s}^{-1}$ (see the Supporting Information). The ability to pump over this distance and around corners suggests that these types of analyte-responsive, self-powered pumps may be suitable for use in smart devices with complex channel architectures.

Finally, we demonstrated that the TBS-PPHA pumps can be made responsive to specific analytes other than fluoride, which is a critical capability for future applications. For example, Figure 6 shows a reagent (**1**) that responds to the

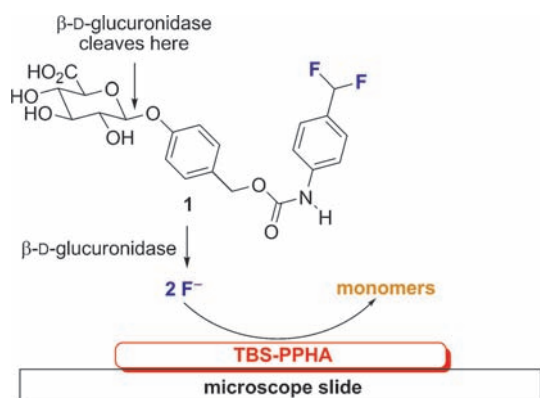


Figure 6. A pump that turns “on” in response to the enzyme β -D-glucuronidase. This type of enzyme-responsive pump requires the TBS-PPHA film and a detection reagent (for example, reagent **1**) that releases fluoride in response to the enzyme.

enzyme β -D-glucuronidase (which is a specific marker of *E. coli*)^[18] by releasing two equivalents of fluoride per enzymatic reaction (Supporting Information, Figure S2). The released fluoride then turns “on” the pump. This system differs from the experiments in Figure 2 and 3 in that the small-molecule reagent (for example, **1**) and the pump must work in concert to provide selective pumping when the enzyme is present. In theory, reagent **1** could be modified easily to create other detection reagents that allow the pump to respond selectively to other analytes as well,^[19] thus providing access to tunable, analyte-selective pumps. To demonstrate this capability, we exposed the TBS-PPHA pump to a 75 mM phosphate-buffered solution (pH 6.8, 1.0 % w/v BSA, 25 °C) that contained 3.1 mM of reagent **1**. In the absence of β -D-glucuronidase, no pumping was observed, but in the presence of $3.1 \mu\text{M}$ β -D-glucuronidase (Supporting Information, Movie S5), the average pumping velocity was $1.3 \pm 0.5 \mu\text{m s}^{-1}$, which is approximately the maximum estimated pumping velocity for the TBS-PPHA pump (Supporting Information, Figure S3 and Movie S5). A control experiment that contained the enzyme but not reagent **1** did not lead to pumping, further confirming that both reagent **1** and TBS-PPHA are needed to create an enzyme-responsive pump (Supporting Information, Movie S5).

In conclusion, we have described a set of single-use, analyte-responsive microscale pumps. These pumps are capable of moving fluids and micrometer-scale particles autonomously with velocities that are dictated by the concentration of the specific analyte that turns “on” the pump. We also demonstrated that the pairing of a small-molecule detection reagent with the responsive pumps offers an opportunity to vary the selectivity of the pump in response to a variety of enzymes or chemical signals. These types of pumps will be useful in diverse applications ranging from microanalysis and microfluidics, to single-use diagnostic devices. Experiments to demonstrate these types of applications are currently in progress.

Received: November 4, 2011

Revised: December 19, 2011

Published online: February 2, 2012

Keywords: depolymerization · diffusiophoresis · microfluidic pumps · molecular devices · sensors

- [1] J. Wang, *ACS Nano* **2009**, *3*, 4–9.
- [2] Y. Hong, M. Diaz, U. M. Córdova-Figueroa, A. Sen, *Adv. Funct. Mater.* **2010**, *20*, 1568–1576.
- [3] a) M. E. Ibele, Y. Wang, T. R. Kline, T. E. Mallouk, A. Sen, *J. Am. Chem. Soc.* **2007**, *129*, 7762–7763; b) A. A. Solovev, S. Sanchez, Y. Mei, O. G. Schmidt, *Phys. Chem. Chem. Phys.* **2011**, *13*, 10131–10135; c) T. R. Kline, W. F. Paxton, Y. Wang, D. Velegol, T. E. Mallouk, A. Sen, *J. Am. Chem. Soc.* **2005**, *127*, 17150–17151.
- [4] a) A. P. Esser-Kahn, N. R. Sottos, S. R. White, J. S. Moore, *J. Am. Chem. Soc.* **2010**, *132*, 10266–10268; b) A. P. Esser-Kahn, S. A. Odom, N. R. Sottos, S. R. White, J. S. Moore, *Macromolecules* **2011**, *44*, 5539–5553; c) A. Sagi, R. Weinstein, N. Karton, D. Shabat, *J. Am. Chem. Soc.* **2008**, *130*, 5434–5435; d) M. A. DeWit, E. R. Gillies, *J. Am. Chem. Soc.* **2009**, *131*, 18327–18334.

- [5] W. Seo, S. T. Phillips, *J. Am. Chem. Soc.* **2010**, *132*, 9234–9235.
- [6] E. M. Purcell, *Am. J. Phys.* **1977**, *45*, 3–11.
- [7] a) J. E. Avron, O. Kenneth, D. H. Oaknin, *New J. Phys.* **2005**, *7*, 234; b) C. M. Pooley, G. P. Alexander, J. M. Yeomans, *Phys. Rev. Lett.* **2007**, *99*, 228103; c) R. Golestanian, A. Ajdari, *Phys. Rev. Lett.* **2008**, *100*, 038101; d) T. R. Kline, J. Iwata, P. E. Lammert, T. E. Mallouk, A. Sen, D. Velegol, *J. Phys. Chem. B* **2006**, *110*, 24513–24521; e) W. F. Paxton, K. C. Kistler, C. C. Olmeda, A. Sen, S. K. St. Angelo, Y. Cao, T. E. Mallouk, P. E. Lammert, V. H. Crespi, *J. Am. Chem. Soc.* **2004**, *126*, 13424–13431; f) W. F. Paxton, A. Sen, T. E. Mallouk, *Chem. Eur. J.* **2005**, *11*, 6462–6470; g) W. F. Paxton, P. T. Baker, T. R. Kline, Y. Wang, T. E. Mallouk, A. Sen, *J. Am. Chem. Soc.* **2006**, *128*, 14881–14888; h) Y. Hong, D. Velegol, N. Chaturvedi, A. Sen, *Phys. Chem. Chem. Phys.* **2010**, *12*, 1423–1435; i) T. Mirkovic, N. S. Zacharia, G. D. Scholes, G. A. Ozin, *Small* **2010**, *6*, 159–167.
- [8] a) V. Lenaerts, P. Couvreur, D. Christiaens-Leyh, E. Joiris, M. Roland, B. Rollman, P. Speiser, *Biomaterials* **1984**, *5*, 65–68; b) R. H. Müller, C. Lherm, J. Herbert, P. Couvreur, *Biomaterials* **1990**, *11*, 590–595.
- [9] H. Ito, C. G. Willson, *Polym. Eng. Sci.* **1983**, *23*, 1012–1018.
- [10] S. A. MacDonald, C. G. Willson, J. M. J. Frechet, *Acc. Chem. Res.* **1994**, *27*, 151–158.
- [11] a) D. C. Smith, *J. Biomed. Mater. Res.* **1971**, *5*, 189–205; b) J. Kreuter, S. N. Mills, S. S. Davis, C. G. Wilson, *Int. J. Pharm.* **1983**, *16*, 105–113.
- [12] a) F. Leonard, R. K. Kulkarni, G. Brandes, J. Nelson, J. J. Cameron, *J. Appl. Polym. Sci.* **1966**, *10*, 259–272; b) C. Limouzin, A. Caviggia, F. Ganachaud, P. Hémerly, *Macromolecules* **2003**, *36*, 667–674.
- [13] P. D. Frymier, R. M. Ford, H. C. Berg, P. T. Cummings, *Proc. Natl. Acad. Sci. USA* **1995**, *92*, 6195–6199.
- [14] R. A. Pavlick, S. Sengupta, T. McFadden, H. Zhang, A. Sen, *Angew. Chem.* **2011**, *123*, 9546–9549; *Angew. Chem. Int. Ed.* **2011**, *50*, 9374–9377.
- [15] P. O. Staffeld, J. A. Quinn, *J. Colloid Interface Sci.* **1989**, *130*, 88–100.
- [16] J. L. Anderson, *Annu. Rev. Fluid Mech.* **1989**, *21*, 61–99.
- [17] J. R. Howse, R. A. L. Jones, A. J. Ryan, T. Gough, R. Vafabakhsh, R. Golestanian, *Phys. Rev. Lett.* **2007**, *99*, 048102.
- [18] L. Fiksdal, I. Tryland, *Curr. Opin. Biotechnol.* **2008**, *19*, 289–294.
- [19] M. S. Baker, S. T. Phillips, *J. Am. Chem. Soc.* **2011**, *133*, 5170–5173.